Volume 58
Number 66
25 August 2022
Pages 9163–9300

ChemComm

Chemical Communications

rsc.li/chemcomm

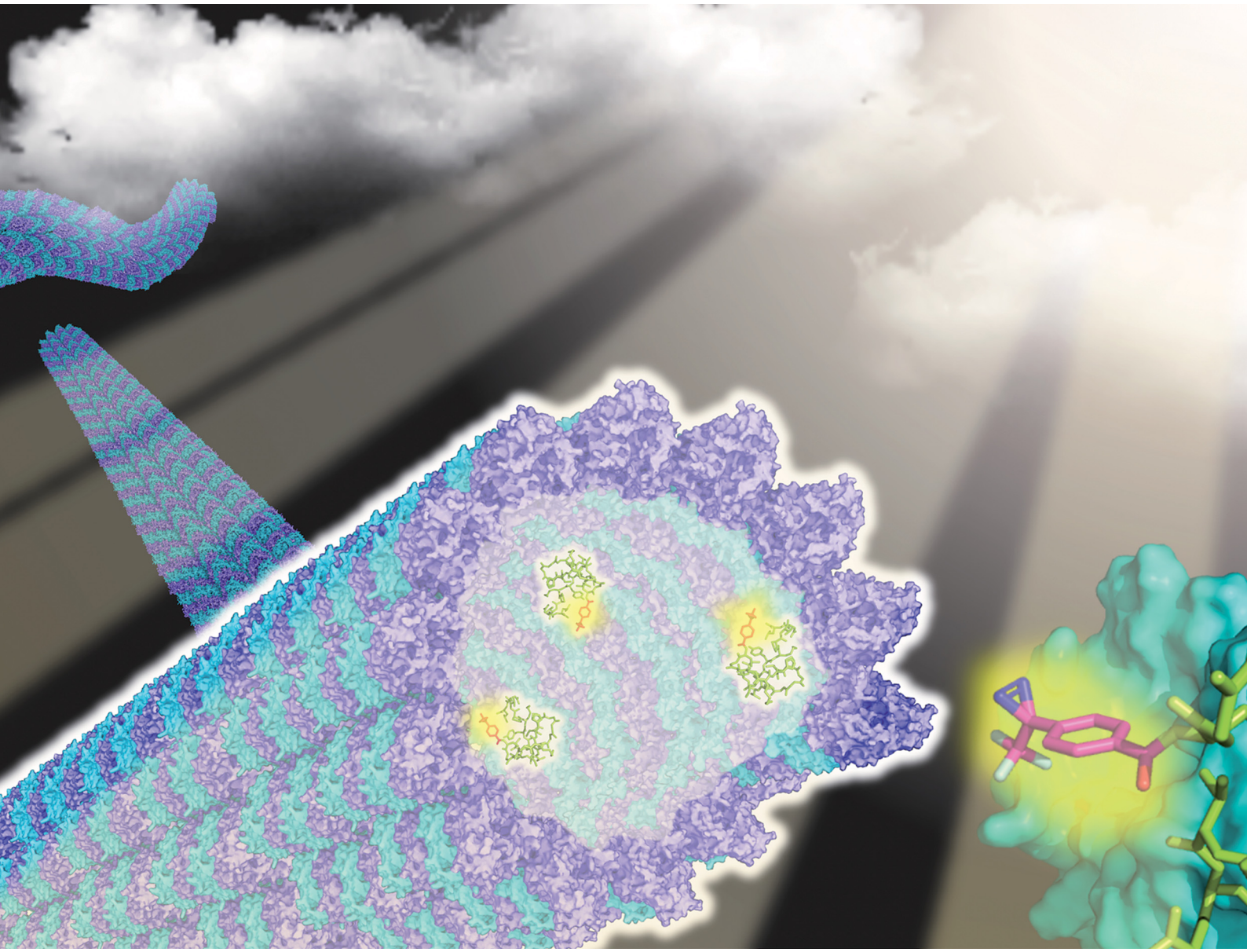

ISSN 1359-7345

ROYAL SOCIETY OF CHEMISTRY

COMMUNICATION

Hiroshi Inaba, Kazunori Matsuura *et al.*
Light-induced stabilization of microtubules by photo-crosslinking of a Tau-derived peptide

ChemComm

COMMUNICATION

View Article Online
View Journal | View Issue

Cite this: *Chem. Commun.*, 2022, **58**, 9190

Received 2nd April 2022,
Accepted 25th July 2022

DOI: 10.1039/d2cc01890j

rsc.li/chemcomm

Light-induced stabilization of microtubules by photo-crosslinking of a Tau-derived peptide†

Soei Watari,[a] Hiroshi Inaba,*[ab] Tomonori Tamura,[c] Arif Md. Rashedul Kabir,[d] Akira Kakugo,[de] Kazuki Sada,[de] Itaru Hamachi[cf] and Kazunori Matsuura*[ab]

For light-induced stabilization of microtubules (MTs) to manipulate cells, a photo-reactive diazirine group was conjugated to a Tau-derived peptide, a motif binding on the inside of MTs. Ultraviolet (UV) light irradiation induced significant stabilization of MTs *via* the formation of a covalent bond of the peptide and showed toxicity.

Microtubules (MTs) are tubular cytoskeletal elements with a 15 nm inner diameter that are formed by the polymerization of tubulin dimers. MTs play important roles in various cell functions such as cell division and shape and intracellular transport, being associated with motor proteins (kinesin and dynein).[1–5] Malfunction of MTs is linked to various pathological conditions, including neurodegenerative diseases, while controlling MT stabilization/destabilization is effective for the treatment of MT-related diseases and cancers.[6–9] Taxol (paclitaxel) is a well-known anticancer drug, which stabilizes MTs by binding to a hydrophobic pocket of β-tubulin inside of the MTs and inhibiting their dynamic instability. However, Taxol has several limitations including a complex synthesis due to its complex structure, low water solubility and side effects resulting from its adverse outcomes on normal cells.[10,11] Gaining spatiotemporal control of the stability and structures of MTs using external stimuli is a promising strategy to manipulate specific cell populations with reduced side effects.[12–19] For example, Thorn-Seshold *et al.* have developed Taxol-azobenzene conjugates that allow control of the structures of intracellular MTs by photoisomerization of the azobenzene moiety.[15] Although photoisomerization is useful for modulating the stabilization of MTs, its reversible property might result in moderate MT stabilization. Thus, we focused on using a photoaffinity labelling technique.[20,21] In this technique, light irradiation converts photoaffinity probes to highly reactive species such as carbene that form covalent bonds with nearby residues among the target proteins. Horwitz *et al.* have developed Taxol-photoaffinity labelling agents to identify the binding site of Taxol and its analogues.[22,23] The Taxol-photoaffinity labelling agents have not been used to control the stability and structures of MTs by light irradiation, probably because of the stabilization of MTs even without light irradiation.

We have previously designed a Tau-derived peptide (**TP**) that binds to the interior hydrophobic pocket of MTs like Taxol.[24] Its sequence (CGGGKKHVPGGGSVQIVYKPVDL) was based on the repeat domain of the MT-associated protein Tau. Using **TP**, we have encapsulated various nanomaterials such as proteins[25,26] and magnetic nanoparticles[27] to modulate the structure and function of MTs.[28] We have also confirmed binding of red fluorescent tetramethylrhodamine (TMR)-labelled **TP** to MTs in living cells.[29] Cyclic **TP** bound to tubulin strongly (K_d = 0.94 μM), promoting the stabilization of MTs compared to **TP** (K_d = 6.0 μM).[30] It is considered that the **TP**-photoaffinity labelling agent could increase the binding affinity of **TP** to tubulin and stabilize MTs by light-induced covalent bond formation. In this study, we have conjugated a photo-reactive diazirine (DA), which forms a carbene upon UV light irradiation,[20,21] at the *N*-terminus of **TP** (**DA-TP**). This strategy allowed stabilization of MTs *via* covalent bond formation upon UV light irradiation *in vitro* and in living cells (Fig. 1). Compared to Taxol-photoaffinity labelling agents[22,23] and Taxol-azobenzene conjugates,[15] **DA-TP** has high water solubility and allows large structural changes of MTs by photoaffinity labeling of DA.

This **DA-TP** was synthesised by Fmoc solid-phase chemistry followed by the introduction of a DA moiety at its N-terminus on the resin (Fig. S1a and S2a, ESI†). The UV-visible spectrum of

[a] *Department of Chemistry and Biotechnology, Graduate School of Engineering, Tottori University, Tottori 680-8552, Japan. E-mail: hinaba@tottori-u.ac.jp, ma2ra-k@tottori-u.ac.jp*
[b] *Centre for Research on Green Sustainable Chemistry, Tottori University, Tottori 680-8552, Japan*
[c] *Department of Synthetic Chemistry and Biological Chemistry, Graduate School of Engineering, Kyoto University, Katsura, Nishikyo-ku, Kyoto 615-8510, Japan*
[d] *Faculty of Science, Hokkaido University, Sapporo 060-0810, Japan*
[e] *Graduate School of Chemical Sciences and Engineering, Hokkaido University, Sapporo 060-0810, Japan*
[f] *JST-ERATO, Hamachi Innovative Molecular Technology for Neuroscience, Nishikyo-ku, Kyoto 615-8530, Japan*

† Electronic supplementary information (ESI) available: Experimental details and supporting figures. See DOI: https://doi.org/10.1039/d2cc01890j

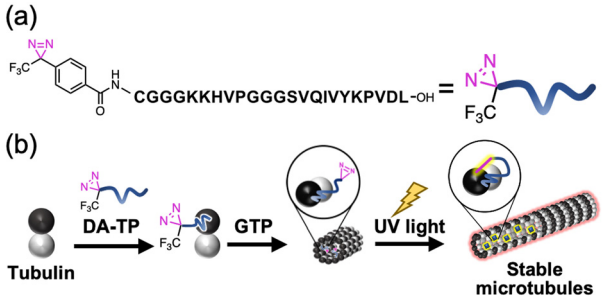

Fig. 1 (a) Structure of the diazirine-conjugated Tau-derived peptide (**DA-TP**) designed in this study. (b) Schematic illustration of our approach involving light-induced stabilization of microtubules (MTs) by incorporation of **DA-TP** and subsequent ultraviolet (UV) light irradiation.

DA-TP changed upon UV light irradiation (Fig. S3, ESI†), confirming the generation of carbene as reported previously.[31] The dissociation constant (K_d) of **DA-TP** to tubulin was estimated as 6.1 μM (Fig. S4, ESI†), by measuring the fluorescence change of the intrinsic tryptophan of tubulin as reported previously.[32] The affinity is similar to that of TMR-labelled **TP** (K_d = 6.0 μM). To evaluate the binding of **DA-TP** to MTs using confocal laser scanning microscopy (CLSM), the cysteine residue of **DA-TP** was modified with TMR (**DA-TP-TMR**) (Scheme S1 and Fig. S1d, S2d, ESI†). The MTs were prepared by preincubation with tubulin, Alexa Fluor 488-labelled tubulin (AF-tubulin) and **DA-TP-TMR**, and subsequent polymerization by guanosine-5′-[(α,β)-methyleno]triphosphate (GMPCPP), a GTP analogue used to form stable MTs (Fig. 2a). The binding of **DA-TP-TMR** to MTs was confirmed by measuring the co-localisation of TMR and AF (Fig. 2b). When Taxol was added to the **DA-TP-TMR**-incorporated MTs, the TMR fluorescence on the MTs was significantly reduced, indicating binding of **DA-TP-TMR** to the interior pocket of the MTs like Taxol. When UV light was applied to the **DA-TP-TMR**-incorporated MTs for 10 min, the TMR fluorescence was not reduced by the addition of Taxol. The amount of **DA-TP-TMR** bound to the MTs was estimated by analysing the fluorescence intensity ratio (I_{TMR}/I_{AF}) from the CLSM images (Fig. 2c). The I_{TMR}/I_{AF} ratio was significantly reduced upon Taxol treatment in the absence of UV light irradiation, while this ratio remained unchanged when UV light irradiation was applied for 10 min. These results indicate a covalent bond formation of **DA-TP-TMR** to the Taxol-binding pocket of the MTs upon UV light irradiation, remaining unaffected by Taxol administration. To further confirm a covalent bond formation between **DA-TP-TMR** and tubulin, SDS-PAGE with fluorescence scanning was performed (Fig. 2d and Fig. S18, ESI†). Following UV light irradiation of the **DA-TP-TMR** and tubulin mixture, TMR fluorescence was observed at the band corresponding to tubulin, contrary to non-UV-irradiated controls. These results confirm a covalent bond formation between **DA-TP-TMR** and tubulin upon UV light irradiation. Molecular mechanics calculations by a MacroModel module predicted the potential binding sites of DA of **DA-TP-TMR** to tubulin (Supporting text and Fig. S5, ESI†).

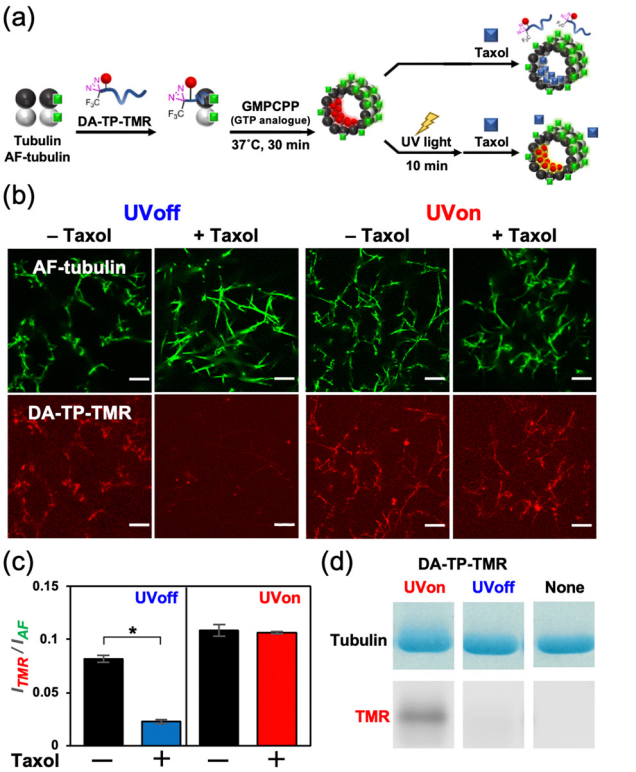

Fig. 2 (a) Schematic illustration showing the incorporation of tetramethylrhodamine (TMR)-labelled **DA-TP** (**DA-TP-TMR**) to GMPCPP MTs, and the competitive binding of Taxol with and without UV light irradiation (365 nm, 52 mW, and 10 min), and (b) resulting confocal laser scanning microscopy (CLSM) images. Preparation concentrations: 10 μM tubulin, 10 μM Alexa Fluor 488-labelled tubulin (AF-tubulin), 40 μM **DA-TP-TMR**, and 100 μM Taxol. Scale bars: 10 μm. (c) Fluorescence intensity ratio (I_{TMR}/I_{AF}) of each **DA-TP-TMR**-bound MT determined from the CLSM images. + and − indicate with and without Taxol, respectively. Error bars represent the standard error of the mean (N = 40). *P < 0.0001, two-tailed Student's t-test. (d) SDS-PAGE and fluorescence scanning results of tubulin incubated with **DA-TP-TMR** with and without UV light irradiation (365 nm, 52 mW, and 20 min) or only tubulin. Preparation concentrations: 10 μM tubulin, 20 μM **DA-TP-TMR**.

The effect of **DA-TP** on the formation efficiency of MTs was estimated using MTs prepared with GTP, which are generally unstable. **DA-TP**-encapsulated MTs were prepared with GTP and the supernatant (tubulin) and pellet (MTs) were separated by ultracentrifugation and analysed by SDS-PAGE to estimate the formation efficiency of MTs (Fig. S6, ESI†). Treatment of **DA-TP** increased the MT formation efficiency (62%) compared to controls without any additive (39%). Following UV light irradiation to the **DA-TP**-encapsulated MTs, the MT formation efficiency further increased (74%) reaching levels similar to Taxol treatment. These results indicate that **DA-TP** stabilizes MTs, while UV light irradiation further enhances its stabilization effect.

Stabilization of GTP MTs by **DA-TP** was further evaluated using CLSM. Although GTP MTs were unstable, with aggregates only observed without additive, **DA-TP** induced the formation of MTs similar to Taxol (Fig. 3a). Conversely, the formation of MTs was not observed when UV light was applied to the mixture

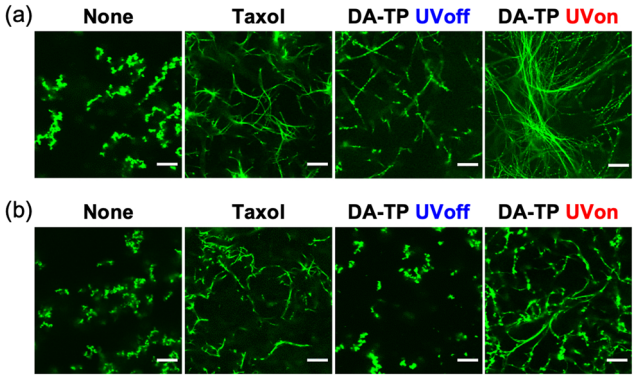

Fig. 3 CLSM images of GTP MTs prepared with **DA-TP**, Taxol or without any additives (a) after polymerization and (b) further incubation at 4 °C for 15 min. UV light was applied for 5 min. Contour and persistence lengths of MTs were determined from CLSM images (Fig. S8g and S9e, ESI†). Preparation concentrations: 2 μM tubulin, 2 μM AF-tubulin, 8 μM **DA-TP** or Taxol. Scale bars, 10 μm.

of tubulin and **DA-TP** after the addition of GTP (Fig. S7, ESI†). Interestingly, UV light irradiation to **DA-TP**-encapsulated MTs induced the formation of longer and more rigid MTs. Analysis of MTs using the CLSM images revealed that applying UV light irradiation to the **DA-TP**-encapsulated MTs increased both their contour length (1.6-fold) and persistence length (1.4-fold), compared to controls without UV irradiation (Fig. S8, ESI†). Under depolymerization conditions of MTs (4 °C), **DA-TP**-encapsulated MTs without UV light irradiation were also completely depolymerized and formed dot-like aggregates (Fig. 3b). By contrast, **DA-TP**-encapsulated MTs exposed to UV light irradiation remained even at 4 °C, while their contour length and persistence length were similar to those of MTs treated with Taxol (Fig. S9, ESI†). Thus, the covalent bond formation between **DA-TP** and MTs induced by UV light irradiation resulted in long, rigid and stable MTs. The increased amount of **DA-TP** triggered by UV light also generated longer and more rigid MTs (Fig. S10, ESI†). Two control peptides (*i.e.*, **TP** modified with DA at different positions and actin-binding peptide, Lifeact, modified with DA) were not bound to the Taxol-binding pocket and showed no effects on the stabilization of MTs with and without UV light irradiation (Supporting text and Fig. S11, S12, ESI†). Thus, the **TP** sequence with a DA at the *N*-terminus is important for the light-induced stabilization of MTs by covalent bond formation.

The motile properties of **DA-TP**-encapsulated GMPCPP MTs driven by ATP on kinesin-coated substrates were next analysed by fluorescence microscopy (Fig. S13, ESI†). The velocity of **DA-TP**-encapsulated GMPCPP MTs increased 1.3 and 1.7-fold, respectively, before and after UV light irradiation compared to control MTs. The persistence length of GMPCPP MTs was also increased by the treatment of **DA-TP** and subsequent UV light irradiation. The increased velocity of GMPCPP MTs was presumably due to an increased rigidity of the MTs as we have reported previously.[23–25]

After confirming the UV light-induced stabilization of the **DA-TP**-encapsulated MTs *in vitro*, the binding of **DA-TP-TMR** to

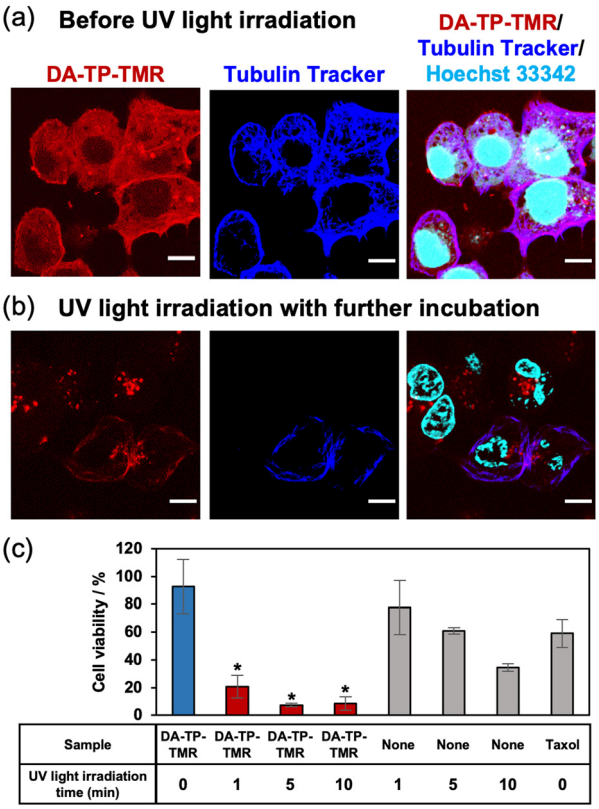

Fig. 4 Effects of **DA-TP-TMR** on HepG2 cells. CLSM images showing HepG2 cells (a) upon introduction of **DA-TP-TMR** and (b) after UV light irradiation (5 min) and further incubation for 15 h. Intracellular MTs were depolymerized by demecolcine and then 10 μM **DA-TP-TMR** was applied to the cells using ProteoCarry. Intracellular MTs were stained with Tubulin Tracker Deep Red and cell nuclei were stained with Hoechst 33342. Scale bars: 10 μm. (c) Toxicity of **DA-TP-TMR** to HepG2 cells. HepG2 cells treated with 10 μM **DA-TP-TMR** or Taxol as above were further incubated for 24 h and their viability was determined using the WST assay. Demecolcine-treated cells were used as standards. Error bars represent the standard deviation (N = 3). *P < 0.05 compared to **DA-TP-TMR** without UV light irradiation or only UV light irradiation for the same duration, two-tailed Student's t-test.

human hepatoma HepG2 cells and the resulting effects on the cells were evaluated. Before introducing **DA-TP-TMR**, demecolcine was applied to the cells to depolymerize intracellular MTs,[33,34] thus allowing for the binding of **DA-TP-TMR** to tubulin and subsequent repolymerization. We confirmed that intracellular MTs were depolymerized by demecolcine and were repolymerized following washing and further incubation (Fig. S14, ESI†). Then, **DA-TP-TMR** was introduced to the demecolcine-treated cells using a protein transfection reagent (ProteoCarry). After incubation for 30 min, co-localisation of **DA-TP-TMR** and Tubulin Tracker was observed, indicating binding of **DA-TP-TMR** to the intracellular MTs (Fig. 4a). When UV light was applied for 5 min to the **DA-TP-TMR**-treated cells, there was no apparent change immediately after the irradiation (Fig. S15, ESI†). However, after a subsequent incubation for 15 h, many cells displayed abnormal shapes with nuclear defects (Fig. 4b). These nuclear defects are hallmarks of cells

treated with MT stabilizers.[15,35] However, the cell abnormalities were not observed when **DA-TP-TMR** was incubated without UV light irradiation (Fig. S16, ESI†). These findings indicate that the binding of **DA-TP-TMR** to intracellular MTs and the stabilization of MTs by UV light irradiation induced the observed cellular abnormalities. The toxicity of **DA-TP-TMR** was further evaluated using the WST assay (Fig. 4c). Viability was greatly reduced in cells treated with **DA-TP-TMR** and UV light irradiation, whereas **DA-TP-TMR** without UV light irradiation had no apparent effect. Although UV light irradiation without **DA-TP-TMR** also showed some cytotoxicity, the combination of **DA-TP-TMR** and UV light irradiation had greater effects. It is suggested that **DA-TP-TMR** bound to MTs in cells combined with UV light irradiation stabilized MTs, thus inhibiting cell proliferation. **DA-TP** and Taxol reduced cell viability in a concentration-dependent manner; however, the tendency was not completely matched (Fig. S17, ESI†). Since the diffusion of **DA-TP-TMR** into the cytoplasm was also observed in the CLSM image (Fig. 4a), it may be possible that parts of **DA-TP-TMR** bind intracellular molecules non-specifically and inhibit their activity by photoaffinity labelling.

In conclusion, we showed that DA-conjugated **TP** formed covalent bonds to MTs and stabilized their structure upon UV light irradiation. Binding of **DA-TP-TMR** to intracellular MTs together with a strong toxicity was observed upon UV light irradiation, indicating that **DA-TP-TMR** can induce MT stabilization within cells. Although Taxol has low water solubility and is difficult to synthesize, **DA-TP** has the advantages of good water solubility and being relatively easy to synthesize. In addition, **DA-TP** can stabilize MTs only when it forms a covalent bond to MTs by photoaffinity labelling. Thus, it is expected that MTs will be stabilized only at the light-exposed areas. This technique will lead to various applications, such as the development of MT-stabilizing drugs with minimal side effects and local cell manipulation. Because prolonged UV light irradiation causes damage to cellular tissues, stabilization of MTs by visible light irradiation is required in the future.

This work was supported by KAKENHI (No. 19K15699 for H. I.) from the Japan Society for the Promotion of Science (JSPS), ACT-X (JPMJAX2012 for H. I.) and FOREST Program (JPMJFR2034 for H. I.) from the Japan Science and Technology Agency (JST).

Conflicts of interest

There are no conflicts to declare.

References

1 A. Desai and T. J. Mitchison, *Annu. Rev. Cell Dev. Biol.*, 1997, **13**, 83–117.
2 E. Karsenti, *Nat. Rev. Mol. Cell Biol.*, 2008, **9**, 255–262.
3 C. Conde and A. Cáceres, *Nat. Rev. Neurosci.*, 2009, **10**, 319–332.
4 A. Akhmanova and M. O. Steinmetz, *Nat. Rev. Mol. Cell Biol.*, 2015, **16**, 711–726.
5 G. J. Brouhard and L. M. Rice, *Nat. Rev. Mol. Cell Biol.*, 2018, **19**, 451–463.
6 M. A. Jordan and L. Wilson, *Nat. Rev. Cancer*, 2004, **4**, 253–265.
7 *The Role of Microtubules in Cell Biology, Neurobiology, and Oncology*, ed. T. Fojo, Humana Press, Totowa, NJ, 2008.
8 S. Manzoor, A. Bilal, S. Khan, R. Ullah, S. Iftikhar, A.-H. Emwas, M. Alazmi, X. Gao, A. Jawaid, R. S. Z. Saleem and A. Faisal, *Sci. Rep.*, 2018, **8**, 3305.
9 M. O. Steinmetz and A. E. Prota, *Trends Cell Biol.*, 2018, **28**, 776–792.
10 C. Dumontet and M. A. Jordan, *Nat. Rev. Drug Discovery*, 2010, **9**, 790–803.
11 C. Janke and M. O. Steinmetz, *EMBO J.*, 2015, **34**, 2114–2116.
12 M. Borowiak, W. Nahaboo, M. Reynders, K. Nekolla, P. Jalinot, J. Hasserodt, M. Rehberg, M. Delattre, S. Zahler, A. Vollmar, D. Trauner and O. Thorn-Seshold, *Cell*, 2015, **162**, 403–411.
13 J. van Haren, R. A. Charafeddine, A. Ettinger, H. Wang, K. M. Hahn and T. Wittmann, *Nat. Cell Biol.*, 2018, **20**, 252–261.
14 R. C. Adikes, R. A. Hallett, B. F. Saway, B. Kuhlman and K. C. Slep, *J. Cell Biol.*, 2018, **217**, 779–793.
15 A. Müller-Deku, J. C. M. Meiring, K. Loy, Y. Kraus, C. Heise, R. Bingham, K. I. Jansen, X. Qu, F. Bartolini, L. C. Kapitein, A. Akhmanova, J. Ahlfeld, D. Trauner and O. Thorn-Seshold, *Nat. Commun.*, 2020, **11**, 4640.
16 L. Gao, J. C. M. Meiring, Y. Kraus, M. Wranik, T. Weinert, S. D. Pritzl, R. Bingham, E. Ntouliou, K. I. Jansen, N. Olieric, J. Standfuss, L. C. Kapitein, T. Lohmüller, J. Ahlfeld, A. Akhmanova, M. O. Steinmetz and O. Thorn-Seshold, *Cell Chem. Biol.*, 2021, **28**(228-241), e6.
17 A. Sailer, J. C. M. Meiring, C. Heise, L. N. Pettersson, A. Akhmanova, J. Thorn-Seshold and O. Thorn-Seshold, *Angew. Chem., Int. Ed.*, 2021, **60**, 23695–23704.
18 L. Gao, J. C. M. Meiring, C. Heise, A. Rai, A. Müller-Deku, A. Akhmanova, J. Thorn-Seshold and O. Thorn-Seshold, *Angew. Chem., Int. Ed.*, 2022, **61**, e202114614.
19 L. Gao, J. C. M. Meiring, A. Varady, I. E. Ruider, C. Heise, M. Wranik, C. D. Velasco, J. A. Taylor, B. Terni, T. Weinert, J. Standfuss, C. C. Cabernard, A. Llobet, M. O. Steinmetz, A. R. Bausch, M. Distel, J. Thorn-Seshold, A. Akhmanova and O. Thorn-Seshold, *J. Am. Chem. Soc.*, 2022, **144**, 5614–5628.
20 F. Kotzyba-Hibert, I. Kapfer and M. Goeldner, *Angew. Chem., Int. Ed. Engl.*, 1995, **34**, 1296–1312.
21 J. Das, *Chem. Rev.*, 2011, **111**, 4405–4417.
22 S. Rao, L. He, S. Chakravarty, I. Ojima, G. A. Orr and S. B. Horwitz, *J. Biol. Chem.*, 1999, **274**, 37990–37994.
23 C.-P. H. Yang, C. Wang, I. Ojima and S. B. Horwitz, *J. Nat. Prod.*, 2018, **81**, 600–606.
24 H. Inaba, T. Yamamoto, A. Md., R. Kabir, A. Kakugo, K. Sada and K. Matsuura, *Chem. – Eur. J.*, 2018, **24**, 14958–14967.
25 H. Inaba, T. Yamamoto, T. Iwasaki, A. M. R. Kabir, A. Kakugo, K. Sada and K. Matsuura, *Chem. Commun.*, 2019, **55**, 9072–9075.
26 H. Inaba, Y. Sueki, M. Ichikawa, A. M. R. Kabir, T. Iwasaki, H. Shigematsu, A. Kakugo, K. Sada and K. Matsuura, *bioRxiv*, 2022, DOI: 10.1101/2022.01.27.476107.
27 H. Inaba, M. Yamada, Mst R. Rashid, A. Md. R. Kabir, A. Kakugo, K. Sada and K. Matsuura, *Nano Lett.*, 2020, **20**, 5251–5258.
28 H. Inaba and K. Matsuura, *Bull. Chem. Soc. Jpn.*, 2021, **94**, 2100–2112.
29 H. Inaba, T. Yamamoto, T. Iwasaki, A. Md., R. Kabir, A. Kakugo, K. Sada and K. Matsuura, *ACS Omega*, 2019, **4**, 11245–11250.
30 H. Inaba, M. Nagata, K. Juliano-Miyake, A. M. R. Kabir, A. Kakugo, K. Sada and K. Matsuura, *Polym. J.*, 2020, **52**, 1143–1151.
31 T. Seifert, M. Malo, J. Lengqvist, C. Sihlbom, E. M. Jarho and K. Luthman, *J. Med. Chem.*, 2016, **59**, 10794–10799.
32 P. Mondal, G. Das, J. Khan, K. Pradhan, R. Mallesh, A. Saha, B. Jana and S. Ghosh, *ACS Chem. Neurosci.*, 2019, **10**, 2609–2620.
33 S. Dutertre, M. Ababou, R. Onclercq, J. Delic, B. Chatton, C. Jaulin and M. Amor-Guéret, *Oncogene*, 2000, **19**, 2731–2738.
34 G. E. Davey, P. Murmann, M. Hoechli, T. Tanaka and C. W. Heizmann, *Biochim. Biophys. Acta*, 2000, **1498**, 220–232.
35 T. J. Mitchison, *Mol. Biol. Cell*, 2012, **23**, 1–6.